Eur. Phys. J. A **16**, 447–456 (2003)
DOI 10.1140/epja/i2002-10109-6

THE EUROPEAN PHYSICAL JOURNAL A

Spontaneous-fission decay properties and production cross-sections for the neutron-deficient nobelium isotopes formed in the ^{44,48}Ca + ^{204,206,208}Pb reactions

A.V. Belozerov[1], M.L. Chelnokov[1], V.I. Chepigin[1], T.P. Drobina[1], V.A. Gorshkov[1], A.P. Kabachenko[1], O.N. Malyshev[1], I.M. Merkin[1], Yu.Ts. Oganessian[1], A.G. Popeko[1], R.N. Sagaidak[1], A.I. Svirikhin[1], A.V. Yeremin[1,a], G. Berek[2], I. Brida[2], and Š. Šáro[2]

[1] Flerov Laboratory of Nuclear Reactions, JINR, 141980 Dubna, Russia
[2] Comenius University, SK-84215 Bratislava, Slovakia

Received: 26 July 2002 / Revised version: 16 October 2002 /
Published online: 18 March 2003 –
Communicated by J. Äystö

Abstract. Heavy-ion fusion reactions ^{48}Ca + ^{204}Pb and ^{44}Ca + ^{208}Pb leading to the same compound nucleus ^{252}No* were run in attempts to produce new neutron-deficient spontaneous-fission isotopes of ^{249,250}No using the electrostatic separator VASSILISSA. Production cross-sections for the spontaneous-fission activities with the half-lives 5.6 and 54 μs observed in these reactions are compared with the measured ones for the well-known isotopes of $^{251-255}$No formed in the heavy-ion fusion reactions ^{48}Ca + ^{206}Pb and ^{48}Ca + ^{208}Pb. The obtained excitation functions for the reaction products formed after the evaporation of 1–4 neutrons from the corresponding compound No nuclei have been compared with similar data obtained earlier and results of statistical model calculations.

PACS. 21.10.Dr Binding energies and masses – 23.60.+e Alpha decay – 25.70.-z Low and intermediate energy heavy-ion reactions – 25.85.Ca Spontaneous fission

1 Introduction and motivation

In the region of transfermium elements, where the macroscopic component of fission barriers decreases to zero, the nuclear shell structure acquires special importance for the nuclear stability. Experimentally, the influence of the $N = 152$ subshell on the spontaneous-fission (SF) half-lives is strikingly manifested for the even Cf, Fm and No isotopes (fig. 1). Recent discoveries of the neutron-deficient SF isotopes of ^{237,238}Cf [1], ^{254}Rf [7] and ^{250}No [2] show that nuclear stability decreases very rapidly with distance off $N = 152$ to the neutron-deficient side. The drastic fall in the half-life values on both sides off the subshell was explained by a decrease in the outer fission barrier below the ground state [10,11]. Later, a different explanation of this phenomenon which is connected with the lower inertia was proposed [12]. These early calculations [11,12] gave no enhancement in the fission stability near the next deformed shell at $N = 162$, later revealed experimentally [13,14] and theoretically [15–18]. Despite remarkable progress in the calculations, the accuracy in the predicted half-lives still leaves much to be desired, particularly in respect to the predictions for odd nuclei and their use in planning the experiments.

In this regard, a linear (in log scale) extrapolation (see fig. 1) shows that synthesis of the next even isotope of No with $N = 146$ becomes questionable. At the same time, the data for the odd nuclei show a remarkable increase in their stability due to the effective growth of their fission barriers caused by an odd neutron. The increase in stability for odd nuclei is usually expressed by a hindrance factor in relation to neighboring even nuclei. For the considered region this factor is close to 10^4. It allows us to hope that ^{249}No can be detected using the VASSILISSA recoil separator [19].

Fusion-evaporation reactions of ^{44,48}Ca with Pb target nuclei seem to be the most suitable for synthesizing the neutron-deficient isotopes of No. These reactions occupy a special place among the so-called "cold"-fusion reactions induced by lighter and heavier projectiles. Investigations undertaken by different groups [2,20–26] during more than 20 years have led to compatible results in the measured cross-section values for evaporation residues (ER) produced in these reactions. The obtained values are about two orders of magnitude higher than those for Rf isotopes with the same neutron numbers produced in

[a] e-mail: eremin@sunvas.jinr.ru

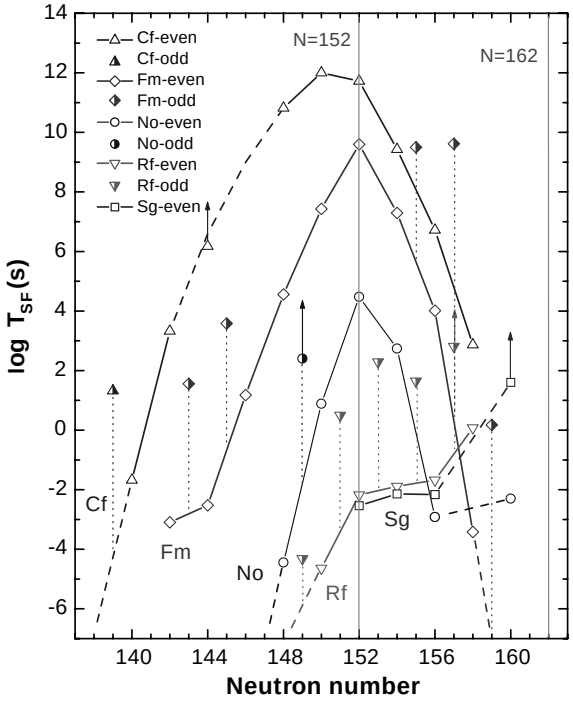

Fig. 1. Partial SF half-lives for even-even and even-odd nuclei from Cf to Sg. Experimental data are taken from [1,2] (^{237,238}Cf, ^{250}No), [3] (^{251}No), [4–6] (^{262}Rf, ^{266}Sg), [7] (^{253,254}Rf, ^{258}Sg), [8] (^{262}Sg) and [9] (for the rest of the nuclei).

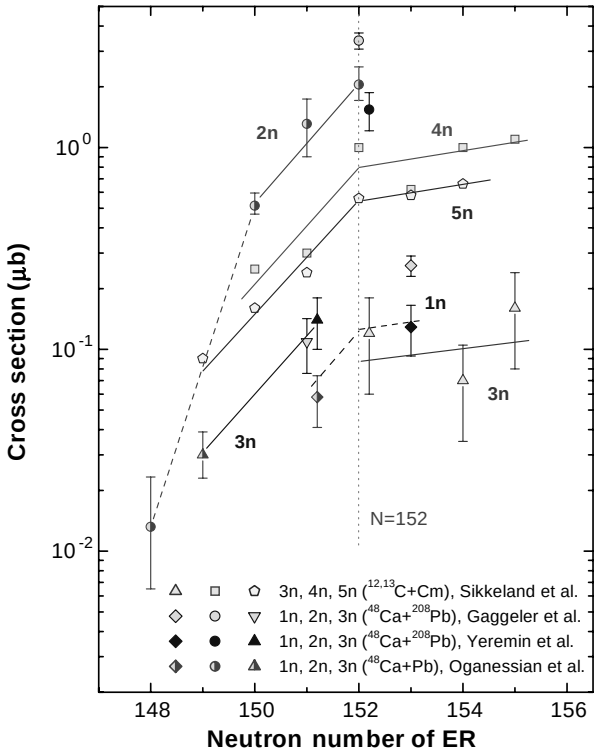

Fig. 2. Cross-section values at the maxima of the excitation functions for the production of No isotopes in the ^{48}Ca + Pb [2,25,26] and ^{12,13}C + Cm [32] reactions as a function of the neutron number of produced nuclei (ER). Tendencies in the change of the dependences at crossing the $N = 152$ subshell are shown by straight lines drawn to guide the eye through the points corresponding to the same evaporation channel.

the ^{50}Ti + Pb reactions [7]. Moreover, these values are greater than those for Fm isotopes with smaller neutron numbers produced in the ^{40}Ar + Pb reactions [27–29]. The latter can be explained by the difference in the compound-nucleus (CN) excitation energy at the fusion (Bass) barrier [30], $E^*_{\rm CN}(B_{\rm Bass})$, which leads to an extra-step in the evaporation cascade for the ^{40}Ar + Pb reactions ($E^*_{\rm CN}(B_{\rm Bass}) \sim 30$ MeV) in comparison with $E^*_{\rm CN}(B_{\rm Bass}) \sim 20$ MeV for the ^{48}Ca + Pb reactions [31]. Our preliminary analysis shows that a similar situation should be the case in the ^{48}Ca + ^{204}Pb ($E^*_{\rm CN}(B_{\rm Bass}) =$ 22.8 MeV) and ^{44}Ca + ^{208}Pb ($E^*_{\rm CN}(B_{\rm Bass}) = 30.4$ MeV) reactions planned to be used for the synthesis of the neutron-deficient No isotopes.

One has to keep in mind that ^{48}Ca + Pb reactions lead to the production of No isotopes around the deformed neutron shell at $N = 152$. The influence of this subshell is clearly manifested in the cross-section values for No isotopes produced in "hot"-fusion reactions of ^{12,13}C with Cm target nuclei [32]. In fig. 2 these data are shown as a function of the neutron number of the produced nucleus (ER). The available data on the production of No isotopes in the ^{48}Ca + Pb reactions [2,25,26] reveal the same tendency as we have seen in the same figure.

So, the nuclear shell structure is of special importance not only for the stability of nuclei in their ground state, but also for their survival in complete fusion reactions. In this regard, a strong deviation of the measured cross-section for ^{250}No produced in the ^{204}Pb(^{48}Ca, 2n) reaction [2] from the extrapolated value has attracted our attention.

In the present work, we report on the results obtained in experiments aimed at the synthesis of the neutron-deficient ^{249,250}No nuclei using the ^{48}Ca + ^{204}Pb and ^{44}Ca + ^{208}Pb reactions. The ^{48}Ca + ^{206}Pb and ^{48}Ca +^{208}Pb reactions used for tests of the new detector system and calibrations are also considered here and compared with previously obtained results in the course of the analysis of the cross-section data.

2 Experiment

Beams of ^{44,48}Ca were delivered by the FLNR Dubna U400 cyclotron. Enriched Ca material was used for loading the ECR-4M ion source. A continuous beam was used in the experiments. The intensity of the beam passing through the separator targets was typically (0.8–1.5)$\times 10^{12}$ s^{-1}.

The projectile energy was varied by extracting the beam from the appropriate radius of the cyclotron and with the use of Al and Ti degraders installed in front of the target. The beam energy was determined by measuring the energy of the ions scattered at 30° in a thin (200 μg/cm^2)

Au foil and with a time-of-flight technique. The measured energy spread of the scattered ions was $\sim 1\%$ (FWHM).

Enriched lead materials were used for the preparation of the targets, the material enrichment in % was as follows: ^{204}Pb – 99.6 (^{206}Pb – 0.35, ^{207}Pb – 0.02 and ^{208}Pb – 0.03), ^{206}Pb – 97.0 (^{207}Pb – 1.96 and ^{208}Pb – 1.02), ^{208}Pb – 97.2 (^{206}Pb – 1.0 and ^{207}Pb – 1.8). Two targets of ^{206}Pb and ^{208}Pb with average thicknesses of 205 μg/cm^2 and 245 μg/cm^2, respectively, were fabricated by evaporation of metal onto the 0.8 mg/cm^2 Al backing foils. Two targets of ^{204}Pb and ^{208}Pb with average lead thickness of 230 μg/cm^2 and 350 μg/cm^2, respectively, were fabricated by chemical precipitation of a PbS compound onto the 0.74 mg/cm^2 Ti backing foils. Each target consisted of six arc segments, 5 cm^2 in area with an angular extension of 60° and an average radius of 60 mm. The segments of the same isotope and quality were mounted on a disk rotating perpendicularly to the beam direction.

The produced evaporation residues were separated in flight by the VASSILISSA electrostatic separator [19]. The time of flight of ER through the separator was about 2 μs. The separator was upgraded to provide an additional suppression of unwanted reaction products and ensure the mass resolution within (1.5–2)% for the heaviest nuclei with masses in the region of 250–300 amu [33]. A new dipole magnet with a deflection angle of 37° degrees, was installed behind the separator instead of the old 8° magnet.

For the registration of heavy ER in the focal plane of the dipole magnet, a new system with a 32-strip detector assembly, 60×120 mm^2 in size, and surrounded by backward detectors was developed. Each strip in the focal plane assembly is position sensitive in the longitudinal direction. The position resolution along each strip was measured using the test ^{48}Ca + ^{174,176}Yb and ^{48}Ca + ^{206,208}Pb reactions. The value of 0.5 mm (FWHM) was obtained for sequential α-α decays, 0.8 mm for ER-α and 1.0 mm for ER-SF events. These values were obtained for energies of the implanted ER in the range from 4 to 15 MeV. A typical energy resolution of about 20 keV for the focal plane detector was obtained for α-particles in the energy range from 6 to 9 MeV. In the case of backward detectors, we obtained the energy resolution of about 150 keV. The reason for that is a broader range of energy losses for escaping α-particles hit into the backward detectors over a wide range of angles.

In our data acquisition system each recorded event corresponds to the energy, position and time of a signal arising inside the detector. All the analog signals were coming to the 8-channel multiplexers and after that were converted by ADCs independently for the ER-, α- and SF-signals. Thus, the dead time between ER and SF detection was close to zero. The time differences between the consequent ER-, α- and/or SF-events of the decay chain were measured within a coincidence time of 1 μs, corresponding to the accuracy of time counters and shaping time of amplifiers. The data transfer and acquisition system of VASSILISSA were described earlier in detail in [34].

3 Results and discussion

3.1 SF decay properties of the neutron-deficient ^{249,250}No isotopes

3.1.1 The ^{48}Ca + ^{206,208}Pb reactions

The ^{206,208}Pb targets were used to check the transmission of the separator, as well as for energy and position calibrations of the focal plane detector assembly. In the ^{48}Ca + ^{206}Pb reaction, at the beam energy of $E_{\rm lab}$ = (210.5 ± 2.1) MeV (here and below we mention the value at the half-thickness of the target) 74 ER-SF and 54 ER-α events were detected and assigned to the decay of ^{252}No. The half-life determined on the basis of the procedure usually employed in the case of poor statistics [35] was obtained as $T_{1/2} = (2.38^{+0.26}_{-0.22})$ s. This agrees with the earlier reported values: (2.44 ± 0.04) s [2] and (2.30 ± 0.22) s [9]. The SF branching ratio for ^{252}No was estimated to be $b_{\rm SF}$ = (32 ± 3)% which is comparable with the values obtained earlier: (32.2 ± 0.5)% [2] and (26.9 ± 1.9)% [9]. Several SF and α events assigned to ^{252}No were detected in the ^{48}Ca + ^{208}Pb reaction, at beam energies of (229.7 ± 2.3) (236.6 ± 2.4) MeV. It allowed us to estimate cross-section values for the ^{208}Pb(^{48}Ca,4n) reaction (see below). Earlier we obtained only the upper limit of the cross-section value for this evaporation channel [26].

In the ^{48}Ca + ^{206}Pb reaction, at the beam energy of $E_{\rm lab}$ = (234.5 ± 2.3) MeV, two ER-SF events with absolute values of time differences between the implantation of ER and SF of 8 μs and 9 μs were detected. The half-life for these events corresponds to $(5.9^{+10.7}_{-2.3})$ μs and can be tentatively assigned to the decay of ^{250}No formed in the 4n evaporation channel (see further results for this activity below). Earlier, the half-life values for this isotope were reported to be (36^{+11}_{-6}) μs [2] and (250 ± 50) μs [36].

3.1.2 The ^{48}Ca + ^{204}Pb reaction

The ^{204}Pb target was irradiated with ^{48}Ca at four beam energies $E_{\rm lab}$ = 217.8, 223.6, 229.4 and 236.1 MeV. At the first three energies the total of 72 ER-SF events were detected. These events were distributed in three groups according to their ER-SF time differences as can be seen in fig. 3. The fitting procedure with the use of the formalism [35] yields three half-life values which are equal to $T_{1/2} = (5.9^{+1.1}_{-0.8})$ μs (42 events), $(54.2^{+14.7}_{-9.5})$ μs (22 events) and $(2.4^{+1.1}_{-0.6})$ s (10 events).

We assigned the events with the half-life $T_{1/2}$ = 2.4 s to the decay of ^{252}No produced in the reaction of ^{48}Ca on the ^{206}Pb contamination in the ^{204}Pb target. The events with the half-life $T_{1/2}$ = 5.9 μs could be assigned to the decay of ^{250}No, whereas the events with the half-life $T_{1/2}$ = 54.2 μs could be tentatively assigned to the decay of the lightest odd isotope ^{249}No. Such identification was based on the comparison of the observed yields for the 6 μs and 54 μs SF activities with the measured and calculated excitation

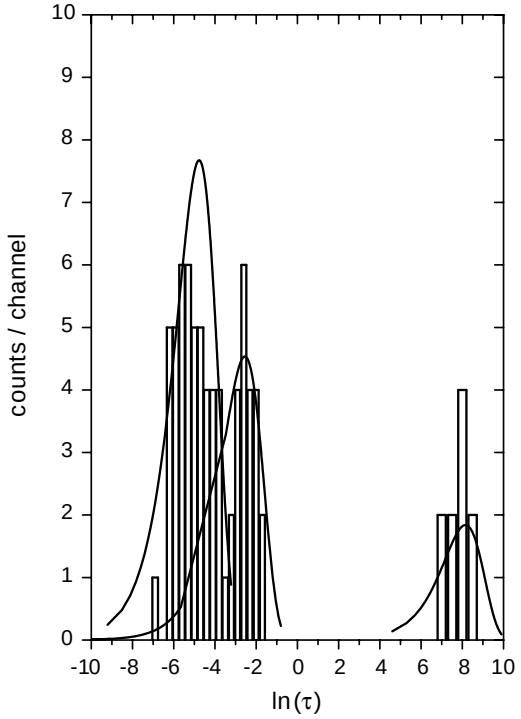

Fig. 3. The logarithm of the ER-SF time differences (in ms), $\ln(\tau)$, for ER-SF correlated events collected in the irradiations of the ^{204}Pb target with ^{48}Ca.

functions for the ^{48}Ca(Pb, xn) reactions and will be considered in detail in the next section.

No ER-α-α correlations corresponding to the decay of the ^{250}No isotope into the well-known ^{246}Fm and ^{242}Cf daughter nuclei as well as for that of the ^{249}No isotope into the ^{245}Fm and ^{241}Cf daughter nuclei were detected. Proceeding from the non-observation of such correlations the upper limits for the α-branching ratio have been estimated as $b_\alpha < 10\%$ and $b_\alpha < 20\%$ for the ^{250}No and ^{249}No, respectively.

At the highest beam energy $E_{\rm lab} = 236.1$ MeV, when ^{248}No could be observed as a result of the 4n evaporation, the integral flux of 7×10^{16} ions was collected and no SF events were detected. It corresponds to the upper limit of the production cross-section value ~ 0.2 nb (for nuclei with $T_{1/2} \geq 2$ μs and for the observation of one decay). In the case of SF of nuclei ($T_{1/2} \lesssim 2\mu$s) in flight through the separator, ER will not reach the focal plane detectors and will be lost. If ER undergo a fast α-decay in flight, the probability that the daughter nucleus will reach the focal plane detector is decreased by the factor of 5–10 as compared with a non-decaying (relatively long-lived) nucleus. The daughter nucleus ^{244}Fm undergoes spontaneous fission with $T_{1/2} = 3$ ms. Taking into account the relatively low value (about 0.5 nb) of the cross-section estimated for the 4n evaporation channel (see the next section) and the time of flight of ER through the separator (about 2 μs), we estimate on the basis of the non-observation of the SF decay the upper limit for the half-life of ^{248}No as $T_{1/2} < 2$ μs.

Table 1. SF decay properties of the neutron-deficient nobelium isotopes resulted in the ^{44,48}Ca + ^{204,206}Pb reaction studies.

Isotope	Number of events	$T_{1/2}^{(\rm SF)}$ (μs)	b_α (%)
^{250}No	56	$5.6^{+0.9}_{-0.7}$	< 10
^{249}No	24	$54.0^{+13.9}_{-9.2}$	< 20
^{248}No	–	< 2	–

3.1.3 The ^{44}Ca + ^{206,208}Pb reactions

The ^{208}Pb target was irradiated with ^{44}Ca ions at three beam energies: 216.8, 212.1 and 205 MeV, and the ^{206}Pb target was irradiated at the beam energy 214.7 MeV. In the ^{44}Ca + ^{208}Pb reaction, the total of 13 ER-SF events were detected. These events could be distributed into two groups according to their ER-SF time differences, with half-life values equal to $T_{1/2} = (5.4^{+2.3}_{-1.3})$ μs (11 events) and $T_{1/2} = (48^{+87}_{-19})$ μs (2 events corresponding to the 68 and 71 μs ER-SF time differences). These values are in agreement with the similar data obtained in the ^{48}Ca + ^{204}Pb reaction.

In the ^{44}Ca + ^{206}Pb reaction, at the beam energy $E_{\rm lab}$ = 214.7 MeV, when ^{248}No produced in the 2n evaporation channel could be observed, the integral flux of 1.3×10^{17} ions was collected and 1 SF event was detected with the ER-SF time difference of 29 μs. This event can be assigned to ^{250}No produced in the reaction of ^{44}Ca with the ^{208}Pb contamination in the ^{206}Pb target. The upper limit of the cross-section value for the production of ^{248}No is about 0.1 nb (if $T_{1/2} \geq 2$ μs). This value is less than that estimated with the use of our data for the ^{208}Pb(^{44}Ca, 2n) reaction (about 0.5 nb too). Thus, the upper limit for the half-life of ^{248}No, as in the previous case, does not exceed the value of 2 μs, the time of flight of ER through the separator.

3.1.4 Comparison of No SF decay properties with calculations, extrapolations and previous results

From the data collected in all our Ca + Pb irradiations we determined the SF decay properties of the neutron-deficient isotopes of Nobelium as presented in table 1.

The calculated alpha-decay properties of the ^{248}No and ^{250}No isotopes are as follows: $Q_\alpha = 9.28$ MeV and 8.99 MeV and $T_\alpha = 21$ ms and 160 ms, respectively [16]. As for the calculated $T_{\rm SF}$ values, estimates performed in the framework of a dynamical approach [15] lead to the values corresponding to 0.5 μs and 15 μs for ^{248}No and ^{250}No, respectively [37].

The obtained results are in agreement with the linear (in log scale) extrapolation of the $T_{\rm SF}$ values for the neutron-deficient even and odd (keeping in mind the hindrance factor of $\sim 10^4$) No isotopes (see fig. 1).

To explain the difference in the results of our work and previous studies [2,36] it is necessary to bear in mind

that there were considerable dead-time intervals in the detection of SF activities. Thus, in the early work [36] the complete fusion ^{233}U(^{22}Ne, 5n) reaction and rotating-wheel technique with mica detectors for the detection of SF events were used. A time interval for the observation of the SF activity decay corresponded to 0.1–2.5 ms. In the recent work [2], the complete fusion-evaporation ^{206}Pb(^{48}Ca, 4n) and ^{204}Pb(^{48}Ca, 2n) reactions were studied with the use of the gas-filled recoil separator. The dead time of 84 μs of the electronic systems used in these measurements [2], as in the previous case [36], did not allow one to detect any SF activities with $T_{1/2} < 10$ μs.

3.1.5 Mass estimates for the observed SF activities

We attempted to identify the observed SF activities more definitely using mass determination with the 37° dipole magnet. The basic relations for the mass determination are as follows: $B\rho \sim \sqrt{A \cdot E}/Q$ and $E \sim A \cdot v^2$, where $B\rho$, A, E, Q and v are the magnetic rigidity, mass, energy, ion charge and velocity of the detected ER. Combining these relations, one can get the expression for the mass determination: A(atomic mass number)/Q(ion charge number) = 9.6525 $\cdot B\rho$(T·m)/v(cm/ns). Thus, we have to measure the velocity or time-of-flight (TOF) and magnetic rigidity (position on the focal plane) for the implanted ER having the ion charge Q. In these coordinates ($B\rho$-TOF) different ion charge numbers of ER are well resolved.

An ability of the system to determine the masses was tested using ^{198}Po produced in the ^{164}Dy(^{40}Ar, 6n) reaction and ^{246}Fm produced in the ^{208}Pb(^{40}Ar, 2n) reaction. The data were collected in the reference list mode and after their sorting the "magnetic rigidity (strip number)-TOF" distributions for the implanted and decaying nuclei were derived [33].

A similar procedure was applied to the data collected in the Ca + Pb studies. Using ER-SF correlations, the positions of the implanted ER and the corresponding TOFs (attributed to a certain SF decay half-life) were extracted. The results are shown in fig. 4. For all the observed SF activities the most probable atomic mass values for the most probable charge states were found by solving the system of equations for A/Q values by the maximum likelihood method. These values correspond to our simulation based on the approximations describing the energy and charge distributions for ER [38,39]. The results of the fit are shown in table 2 where the atomic mass numbers corresponding to the assumed charge states of ER are given for the observed SF activities. The mean weighted values of the numbers are also given in table 2.

One can mention, that an offset in the charge states per one unit of charge to the higher or lower states leads to essential overestimates and underestimates, respectively, in the mass numbers within about ±10 units. So, one can conclude that averaged masses of the observed SF activities are not far from masses of compound nuclei formed in corresponding reactions and masses of nuclei produced in the few-nucleon evaporation channels.

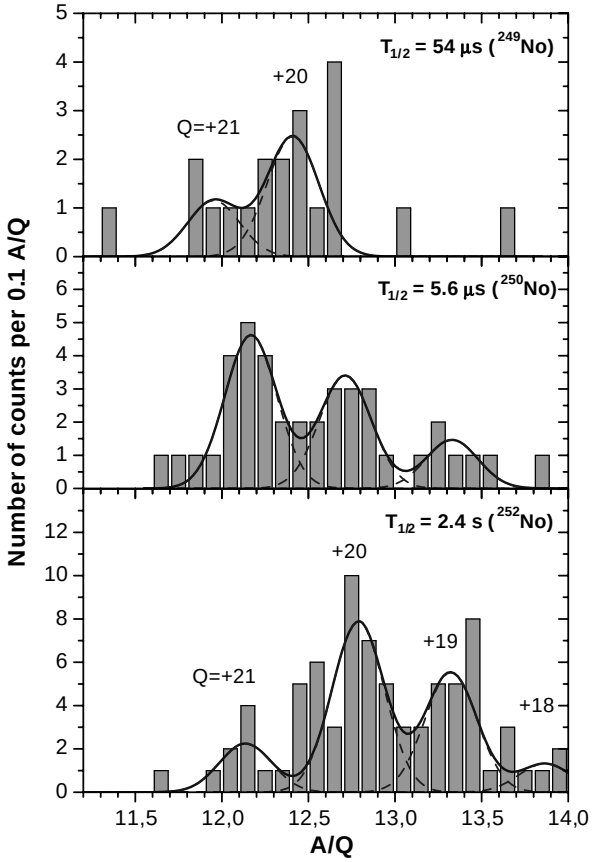

Fig. 4. A/Q distributions for the 5.6 μs, 54 μs and 2.4 s SF activities observed in the ^{44,48}Ca + ^{204,206}Pb reactions (histograms) and the results of a joint multi-Gaussian fit to the data (lines). Assumed charge states for ER are designated in the upper and bottom panels.

Table 2. Atomic mass numbers of the SF activities observed in the ^{44,48}Ca + ^{204,206}Pb reactions.

Charge state	^{249}No	^{250}No	^{252}No
18			249.6±2.4
19		253.3±1.8	253.1±0.8
20	248.2±1.5	254.3±1.1	255.8±0.7
21	251.0±2.9	255.5±0.9	254.9±1.3
Averaged mass	248.8±1.3	254.8±0.7	254.5±0.9

3.2 Excitation functions

Below we analyze our cross-section data obtained in the course of present experiments together with the most recent data [2,25,26] obtained in the ^{48}Ca + Pb reaction studies performed using the recoil separators. In our estimates of the cross-section values we used the data on spectroscopy and decay properties for $^{249-255}$No obtained earlier [7,2,3,9] and in the present work. The transmission efficiency of the VASSILISSA separator for ER produced in complete fusion reactions under investigation was estimated using the simulation code described earlier [40] and checked in test reactions.

3.2.1 General features of the model analysis

The analysis was performed in the framework of the potential-barrier penetration (PBP) model coupled with the standard statistical model (SSM) realized in the HIVAP-code (see ref. [31]). Our approach to the analysis of the data and the choice of model parameters is presented in [41]; here we only pay attention to the important details of the analysis.

We remind that the calculated cross-sections for ER at energies well above the fusion barrier [30] are weakly sensitive to the form of the nuclear potential [41]. At these energies they are determined by the SSM parameters describing de-excitation of a CN. We have chosen Reisdorf's formula for the macroscopic parameters of nuclear level density. It leads to the ratio $\tilde{a}_{\rm f}/\tilde{a}_{\nu} \gtrapprox 1$ due to different nuclear shapes in the saddle point and equilibrium state [31]. Ground-state shell effects were taken into account with a damping constant of 18.5 MeV in the level density as proposed earlier [31,42]. The shell effect in the saddle point was neglected. Empirical ground-state masses [43] were used for the calculations of the shell corrections ($\delta W_{\rm gs}$) as a difference between empirical and liquid-drop masses of a nucleus. Ground-state masses [43] were also used to calculate the excitation and particle separation energies. Therefore, the fit of the calculations at high energies was reduced to the choice of only one adjustable parameter $k_{\rm f}$, the scaling factor at the rotating liquid-drop (LD) fission barriers, $B_{\rm f}^{\rm LD}(\ell)$ [44]. In the calculations, the fission barriers were expressed via these values as $B_{\rm f}(\ell) = k_{\rm f} \times B_{\rm f}^{\rm LD}(\ell) - \delta W_{\rm gs}$.

The barrier passing cross-sections were calculated in the framework of the PBP model using the nuclear exponential potential with sharp radii correction, and the fixed parameters of radius $r_0 = 1.12$ fm and diffuseness $d = 0.8$ fm. Fluctuations of the fusion barrier expressed via the radius-parameter percentage, $\sigma(r_0)/r_0$, were generated with a Gaussian distribution of r_0 around its average fixed value. Transmission coefficients were obtained in the framework of the WKB approximation.

For the value of the nuclear potential strength parameter, we used $V_0 = 70$–80 MeV, which seems to be a good choice, at least for the asymmetric reactions with spherical nuclei considered here, as will be seen below. At sub-barrier energies V_0 strongly correlates with the barrier fluctuation parameter $\sigma(r_0)/r_0$ which was also varied. Variations of these parameters allowed us to achieve better agreement of the calculations with the data at the energies below and above the nominal fusion barrier [30].

3.2.2 The ^{208}Pb(^{48}Ca, xn) excitation functions

Excitation functions for the production of No isotopes in the ^{208}Pb(^{48}Ca, xn) reactions are shown in fig. 5. Our new data on the 2n and 3n evaporation channels are in good agreement with the previous measurements [2, 25,26]. As mentioned above, we have also obtained new cross-section data for the 4n evaporation channel as can be seen in the figure. The very low 4n cross-section values, even in comparison with those for the 2n channel at the same energies resembles a similar situation observed in the ^{206}Pb(^{48}Ca, xn) reaction [2]. Such behavior of the excitation function is not reproduced in our "standard" calculations as well as in the previous ones [2].

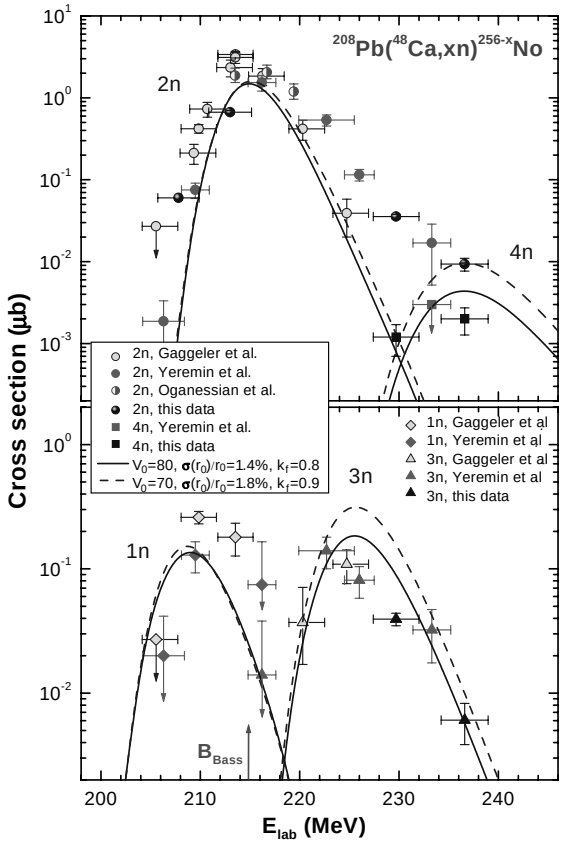

Fig. 5. Excitation functions for the ^{208}Pb(^{48}Ca, xn) reactions, as obtained in this study and earlier works [2,25,26] (symbols), in comparison with the results of calculations with the HIVAP-code [31] (lines).

A drastic drop in the production cross-section values at the maxima of the excitation functions from about 2 μb for the 2n evaporation channel to about 2 nb for 4n has attracted our attention. Such behavior of the excitation functions can be reproduced in calculations within a factor of 2 by a 20% decrease in the LD fission barriers for No nuclei involved in the de-excitation cascade as can be seen in fig. 5. The resulting LD fission barriers are close to the macroscopic ones obtained in the framework of the finite-range model of rotating nuclei [45]. So, no suppression for fusion within an accuracy of and a choice of parameter values in calculations (estimated by the same factor of 2) seems to be observed in the ^{48}Ca + ^{208}Pb reaction (see the further discussion below).

3.2.3 The ^{206}Pb(^{48}Ca, xn) excitation functions

Excitation functions for the production of No isotopes in the ^{206}Pb(^{48}Ca, xn) reactions are shown in fig. 6. In estimates of cross-section values for the 1n evaporation

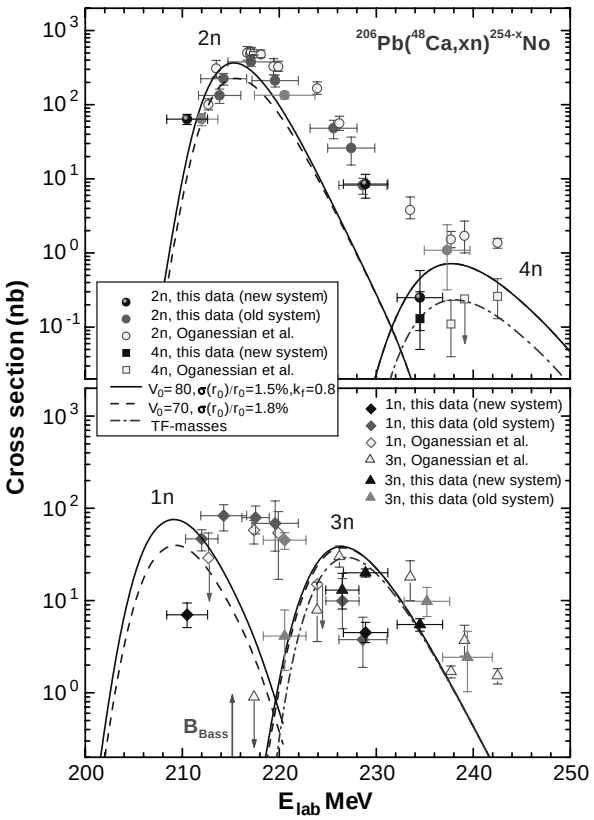

Fig. 6. Excitation functions for the ^{206}Pb(^{48}Ca, xn) reactions obtained in this study and recently [2] (symbols) in comparison with the results of calculations with the HIVAP-code [31] (lines). Data obtained with the 8° (old system) and 37° (new system) dipole magnets are shown by different symbols.

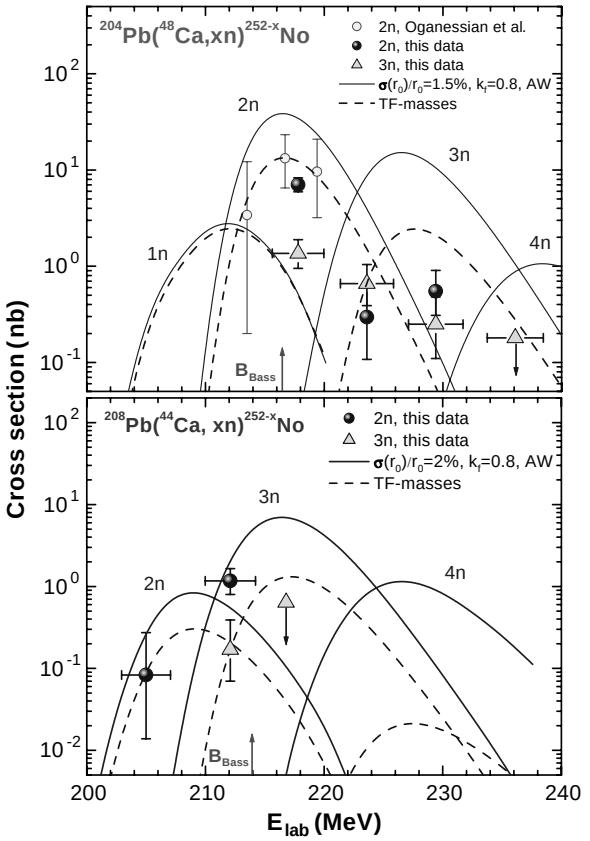

Fig. 7. Cross-sections for the 5.6 μs and 54 μs SF activities produced in the ^{48}Ca + ^{204}Pb and ^{44}Ca + ^{208}Pb reactions leading to the same CN ^{252}No* and assigned to the 2n and 3n evaporation channels, respectively (symbols) in comparison with the calculated excitation functions [31] (lines) and data obtained recently for the 36 μs SF activity [2] (open circles).

channel, a contribution from the 2n product of the reaction on the ^{207}Pb contamination in the target was taken into account using cross-section data obtained recently for the ^{207}Pb(^{48}Ca, 2n) reaction [2]. In these estimates we used the 8.01 MeV α-line (33% of intensity [7]) to distinguish between the 1n channel contribution and that of the ^{208}Pb(^{48}Ca, 2n) reaction leading to ^{254}No (the 8.10 MeV α-line) produced on the ^{208}Pb contamination in the target. The contributions due to ^{207}Pb(^{48}Ca, 3n) and ^{208}Pb(^{48}Ca, 4n) reactions on target impurities yielded their negligible values and were ignored in the estimates of the 2n cross-section values.

As in the previous case, a drastic drop in the production cross-section values at the maxima of the excitation functions from about 0.5 μb for the 2n evaporation channel to about 0.2 nb for 4n has again attracted our attention. Such behavior of the excitation functions *cannot* be reproduced in calculations by a 20% decrease in the LD fission barriers for No nuclei, as was done in the case of the reactions with ^{208}Pb. In this connection, in our further calculations we used the Thomas-Fermi masses [46] for the ^{251}No nucleus and lighter ones. The difference between the Audi-Wapstra [43] and Thomas-Fermi [46] masses for ^{250}No is about 0.5 MeV. It leads to the reduced value of the shell correction to the LD fission barrier in the case of using the Thomas-Fermi mass and to a corresponding drop (more than 3 times) in the production cross-section for ^{250}No as we have seen in fig. 6. So, it seems that there is no need to reduce the damping constant in the level density as well as to introduce the damping (or dependence on the excitation energy) in the fission barriers (see explanations in ref. [47]) as was done in the calculations [2] in attempts to reproduce the data for the ^{206}Pb(^{48}Ca, 4n) reaction.

A noticeable shift corresponding to 6-7 MeV of the maximum of the measured excitation function for the 1n evaporation channel to higher energies in comparison with the results of calculations has also attracted our attention. The same phenomenon was observed in the recent study [2] and so far cannot be explained, at least in the framework of the HIVAP usage.

3.2.4 The ^{204}Pb(^{48}Ca, xn) and ^{208}Pb(^{44}Ca, xn) excitation functions and 5.6 μs and 54 μs SF activities

The obtained cross-section data for the 5.6 μs and 54 μs SF activities are shown in fig. 7. As mentioned above, we assigned these activities to the 2n and 3n evaporation channels leading to ^{250}No and ^{249}No, respectively. In esti-

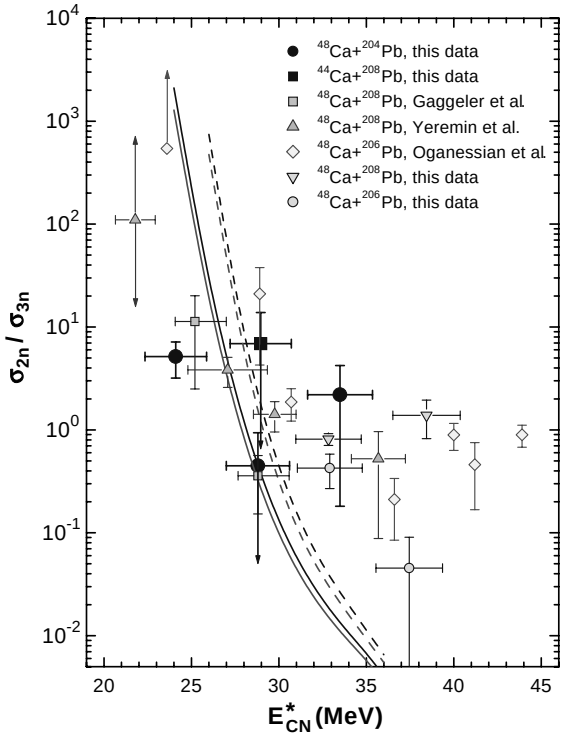

Fig. 8. Cross-section ratios for the 2n and 3n evaporation channels at different CN excitation energies as deduced from this study and [2,25,26] for the ^{48}Ca + ^{206,208}Pb reactions in comparison with the similar data for the 5.6 μs (2n) and 54 μs (3n) SF activities produced in the ^{48}Ca + ^{204}Pb and ^{44}Ca + ^{208}Pb reactions (symbols) and calculations [31] (lines).

mates of the production cross-section values we took into account their time of flight through the separator.

As can be seen in fig. 7, the 5.6 μs SF activity corresponds quite satisfactorily to the calculated excitation function for the 2n evaporation channel of both reactions; whereas the energy dependence for the 54 μs SF activity seems to differ slightly from the one for 5.6 μs activity. It implies a possible SF from an isomeric state for one of them and a SF from the ground state for another one arising from the ^{250}No nucleus. This possibility must not be rejected on the basis of this data. At the same time, the yield of the 54 μs SF activity observed in our ^{48}Ca + ^{204}Pb experiments is an order of magnitude lower than the yield of the 36 μs SF activity observed in similar experiments [2] (see fig. 7), in which the latter was identified as ^{250}No.

To clarify this situation, we considered the ratio of the 2n and 3n cross-section values obtained in this and previous [2,25,26] studies as a function of the CN excitation energy, as shown in fig. 8. As we have seen in the figure, a spread of the data points with the large overlapped errors does not allow us to exclude a possibility of observing the products resulted in the evaporation of 2 and 3 neutrons from the ^{252}No* CN which leads to the 5.6 μs and 54 μs SF activities, respectively. At the same time, as already noted, we cannot exclude unambiguously spontaneous fission from two different states of ^{250}No.

Continuation of the experiments with the ^{44}Ca beam at energies above the fusion barrier seems to be desired for the final identification of the observed SF activities. At the same time, note that the 5.6 μs SF activity corresponds quite well to the calculated 2n evaporation channel for both reactions induced by ^{44}Ca and ^{48}Ca (see fig. 7). The observed suppression in the yield of this activity at the transition from ^{48}Ca to ^{44}Ca is connected with about 8 MeV of the additional excitation energy of the ^{252}No* CN at the nominal fusion barrier [30] due to different reaction Q-values. It makes the (^{44}Ca, 2n) reaction a subbarrier one and resembles a similar suppression of the 2n channel at the transition from ^{48}Ca to ^{40}Ar in the reactions with Pb nuclei.

4 Summary and conclusions

In the course of our experiments aimed at the investigation of the ^{44,48}Ca + ^{204,206,208}Pb reactions, two new short-lived SF activities have been observed. One of them, with the half-life $T_{1/2} = (54^{+14}_{-9})$ μs, seems to be similar to the SF activity, with the half-life $T_{1/2} = (36^{+11}_{-6})$ μs, which was observed in similar experiments performed recently [2]. The yield of the 54 μs SF activity observed in our ^{48}Ca + ^{204}Pb experiments is an order of magnitude lower than the yield of the 36 μs SF activity observed in similar experiments [2], in which the latter was identified as ^{250}No. The second, new SF activity never observed before, has the half-life $T_{1/2} = (5.6^{+0.9}_{-0.7})$ μs and the yield is more than 5 times higher than that for the 54 μs SF activity at the energy corresponding to their maxima production yields. On the basis of the mass measurement with the use of the new dipole magnet as well as using the yields and energy dependences for these activities, we have attributed them to ^{250}No ($T_{1/2} = (5.6^{+0.9}_{-0.7})$ μs) and ^{249}No ($T_{1/2} = (54.0^{+13.9}_{-9.2})$ μs). At the same time, we do not exclude a possible existence of two SF emitters in the case of the ^{250}No nucleus.

Despite some disagreement with the previous work [2], our data confirm a drastic decrease in the nuclear stability with distance off the $N = 152$ deformed neutron shell and correspond to the linear (in log scale) extrapolation of partial SF half-lives to the neutron-deficient side. Such drastic decrease in the nuclear stability can apparently be explained by a corresponding reduction in the shell correction energy for the fission barriers with decreasing N.

Lowering the shell correction energy explains a drastic decrease in the production cross-section values for the neutron-deficient No isotopes observed in the ^{48}Ca + ^{204,206}Pb experiments. The 0.5 MeV reduction in the shell correction energy provided by the Thomas-Fermi nuclear masses leads to general agreement of the calculated cross-section values with the measured ones. The observed suppression of the 5.6 μs SF-activity yield at the transition from ^{48}Ca to ^{44}Ca can be explained by the extra-excitation energy of the ^{252}No* CN at the fusion barrier for the latter.

The technology of centrifugal separation of lead isotopes and receiving highly enriched ^{204}Pb were performed in Russia with the first-hand participation of A.N. Cheltsov (RSC "Kurchatov Institute", Moscow) and V.G. Afanasev (Siberian Chemical Combine, Krasnoyarsk). The authors thank A.N. Shamanin and E.N. Voronkov for the maintenance of the VASSILISSA separator and the U400 crew for providing the stable beams of high intensity. They are thankful to M. Morozova for her help in preparing the manuscript. This work was performed partially under the financial support of the Russian Foundation for Basic Research, contract No. 02–02–16116.

References

1. Yu.A. Lazarev, I.V. Shirokovsky, V.K. Utyonkov, S.P. Tretyakova, V.B. Kutner, Nucl. Phys. A **588**, 501 (1995).
2. Yu.Ts. Oganessian, V.K. Utyonkov, Yu.V. Lobanov, F.Sh. Abdullin, A.N. Polyakov, I.V. Shirokovsky, Yu.S. Tsyganov, A.N. Mezentsev, S. Iliev, V.G. Subbotin, A.M. Sukhov, K. Subotic, O.V. Ivanov, A.N. Voinov, V.I. Zagrebaev, K.J. Moody, J.F. Wild, N.J. Stoyer, M.A. Stoyer, R.W. Lougheed, Phys. Rev. C **64**, 054606 (2001).
3. F.P. Heßberger, S. Hofmann, D. Ackermann, V. Ninov, M. Leino, G. Münzenberg, Š. Šáro, A. Lavrentev, A.G. Popeko, A.V. Yeremin, Ch. Stodel, Eur. Phys. J. A **12**, 57 (2001).
4. Yu.A. Lazarev, Yu.V. Lobanov, Yu.Ts. Oganessian, V.K. Utyonkov, F.Sh. Abdullin, G.V. Buklanov, B.N. Gikal, S. Iliev, A.N. Mezentsev, A.N. Polyakov, I.M. Sedykh, I.V. Shirokovsky, V.G. Subbotin, A.M. Sukhov, Yu.S. Tsyganov, V.E. Zhuchko, R.W. Lougheed, K.J. Moody, J.F. Wild, E.K. Hulet, J.H. McQuaid, Phys. Rev. Lett. **73**, 624 (1994).
5. M.R. Lane, K.E. Gregorich, D.M. Lee, M.F. Mohar, M. Hsu, C.D. Kacher, B. Kadkhodayan, M.P. Neu, N.J. Stoyer, E.R. Sylwester, J.C. Yang, D.C. Hoffman, Phys. Rev. C **52**, 2893 (1996).
6. M. Schädel, W. Brüchle, B. Schausten, E. Schimpf, E. Jäger, G. Wirth, R. Günther, J.V. Kratz, W. Paulus, A. Seibert, P. Törle, N. Trautmann, S. Zauner, D. Schumann, M. Andrassy, R. Miisiak, K.E. Gregorich, D.C. Hoffman, D.M. Lee, E.R. Sylwester, Y. Nagame, Y. Oura, Radiochim. Acta **77**, 149 (1997).
7. F.P. Heßberger, S. Hofmann, V. Ninov, P. Armbruster, H. Folger, G. Münzenberg, H.J. Schött, A.G. Popeko, A.V. Yeremin, A.N. Andreyev, Š. Šáro, Z. Phys. A **359**, 415 (1997).
8. S. Hofmann, F.P. Heßberger, D. Ackermann, S. Antalic, P. Cagarda, S. Ćwiok, B. Kindler, J. Kojoukharova, B. Lommel, R. Mann, G. Münzenberg, A.G. Popeko, Š. Šáro, H.J. Schött, A.V. Yeremin, Eur. Phys. J. A **10**, 5 (2001).
9. R.B. Firestone, V.S. Shirly (Editors), *Table of Isotopes*, 8th ed. (Wiley, New York, 1996).
10. Yu.Ts. Oganessian, in *Symposium on Classical and Quantum Mechanical Aspects of Heavy Ion Collisions, West Berlin, 1974*, *Lect. Notes Phys.*, Vol. **33**, edited by H.L. Harney, P. Braun-Munzinger, C.K. Gelbke (Springer, Berlin, 1974) p. 221.
11. J. Randrup, S.E. Larsson, P. Möller, S.G. Nilsson, K. Pomorski, A. Sobiczewski, Phys. Rev. C **13**, 229 (1976).
12. P. Möller, J.R. Nix, W.J. Świątecki, Nucl. Phys. A **469**, 1 (1987); **492**, 349 (1989).
13. Yu.A. Lazarev, in *XXIV International Workshop on Gross Properties of Nuclei and Nuclear Excitations Extremes of Nuclear Structure, Hirschegg, 1996*, edited by H. Feldmeier, J. Knoll, W. Nörenberg (GSI, Darmstadt, 1996) p. 11.
14. S. Hofmann, Rep. Prog. Phys. **61**, 639 (1998).
15. R. Smolańczuk, J. Skalski, A. Sobiczewski, Phys. Rev. C **52**, 1871 (1995).
16. R. Smolańczuk, A. Sobiczewski, in *XV EPS Nuclear Divisional Conference on Low Energy Nuclear Dynamics, St. Peterburg, 1995*, edited by Yu.Ts. Oganessian, R. Kalpakchieva, W. von Oertzen (World Scientific, Singapore, 1995) p. 313.
17. P. Möller, J.R. Nix, W.D. Myers, W.J. Świątecki, At. Data Nucl. Data Tables **89**, 185 (1995).
18. R. Smolańczuk, Phys. Rev. C **56**, 812 (1997).
19. A.V. Yeremin, A.N. Andreyev, D.D. Bogdanov, G.M. Ter-Akopian, V.I. Chepigin, V.A. Gorshkov, A.P. Kabachenko, O.N. Malyshev, A.G. Popeko, R.N. Sagaidak, Š. Šaro, E.N. Voronkov, A.V. Taranenko, A.Yu. Lavrentev, Nucl. Instrum. Methods Phys. Res. A **350**, 608 (1994); A.V. Yeremin, D.D. Bogdanov, V.I. Chepigin, V.A. Gorshkov, A.P. Kabachenko, O.N. Malyshev, A.G. Popeko, R.N. Sagaidak, G.M. Ter-Akopian, A.Yu. Lavrentev, Nucl. Instrum. Methods Phys. Res. B **126**, 329 (1997).
20. G.N. Flerov, Yu.Ts. Oganessian, A.A. Pleve, N.V. Pronin, Yu.P. Tretyakov, Nucl. Phys. A **267**, 359 (1976).
21. O.A. Orlova, H. Bruchertseifer, Yu.A. Muzychka, Yu.Ts. Oganessian, B.I. Pustylnik, G.M. Ter-Akopian, V.I. Chepigin, Choi Val Sek, Yad. Fiz. **30**, 618 (1979) (Sov. J. Nucl. Phys. **30**, 317 (1979)).
22. J.M. Nitschke, R.E. Leber, M.J. Nurmia, A. Ghiorso, Nucl. Phys. A **313**, 236 (1979).
23. A. Türler, H.W. Gäggeler, D.J. Jost, P. Armbruster, W. Brüchle, H. Folger, F.P. Heßberger, S. Hofmann, G. Münzenberg, V. Ninov, M. Schädel, K. Sümmerer, J.V. Kratz, U. Scherer, Z. Phys. A **331**, 363 (1988).
24. Yu.A. Lazarev, Yu.V. Lobanov, R.N. Sagaidak, V.K. Utyonkov, M. Hussonois, Yu.P. Kharitonov, I.V. Shirokovsky, S.P. Tretyakova, Yu.Ts. Oganessian, Phys. Scr. **39**, 422 (1989).
25. H.W. Gäggeler, D.J. Jost, A. Türler, P. Armbruster, W. Brüchle, H. Folger, F.P. Heßberger, S. Hofmann, G. Münzenberg, V. Ninov, W. Reisdorf, M. Schädel, K. Sümmerer, J.V. Kratz, U. Scherer, M. Leino, Nucl. Phys. A **502**, 561c (1989).
26. A.V. Yeremin, V.I. Chepigin, M.G. Itkis, A.P. Kabachenko, S.P. Korotkov, O.N. Malyshev, Yu.Ts. Oganessian, A.G. Popeko, J. Roháč, R.N. Sagaidak, M.L. Chelnokov, V.A. Gorshkov, A.Yu. Lavrentev, S. Hofmann, G. Münzenberg, Š. Šáro, K. Morita, N. Iwasa, S.I. Mulgin, S.V. Zhdanov, JINR Rapid Commun. No. 6[92]-98, 21 (1998).
27. G. Münzenberg, S. Hofmann, W. Faust, F.P. Heßberger, W. Reisdorf, K.-H. Schmidt, T. Kitahara, P. Armbruster, K. Güttner, B. Thuma, D. Vermeulen, Z. Phys. A **302**, 7 (1981).
28. H. Gäggeler, T. Sikkeland, G. Wirth, W. Brüchle, W. Bögl, G. Franz, G. Herrmann, J.V. Kratz, M. Schädel, K. Sümmerer, W. Weber, Z. Phys. A **316**, 291 (1984).

29. F.P. Heßberger, G. Münzenberg, P. Armbruster, G. Berthes, H. Folger, S. Hofmann, K. Poppensieker, B. Quint, W. Reisdorf, H.J. Schött, K. Sümmerer, I. Zychor, M. Leino, U. Gollerthan, GSI Scientific Report 1986, GSI 87-1, p. 17.
30. R. Bass, Phys. Rev. Lett. **39**, 265 (1977); W. von Oertzen (Editor), *Symposium on Deep Inelastic and Fusion Reactions with Heavy Ions, West Berlin, 1979*, *Lect. Notes Phys.,* Vol. **117** (Springer, Berlin, 1980) p. 281.
31. W. Reisdorf, Z. Phys. A **300**, 227 (1981); W. Reisdorf, M. Schädel, Z. Phys. A **343**, 47 (1992).
32. T. Sikkeland, A. Ghiorso, M. Nurmia, Phys. Rev. **172**, 1232 (1968).
33. Yu.Ts. Oganessian, A.V. Yeremin, A.V. Belozerov, I. Brida, M.L. Chelnokov, V.I. Chepigin, V.A. Gorshkov, S.P. Korotkov, O.N. Malyshev, A.G. Popeko, L.A. Rubinskaya, R.N. Sagaidak, E.M. Smirnova, A.I. Svirikhin, Part. Nucl., Lett. No. 1-[110], 5 (2002).
34. O.N. Malyshev, M.L. Chelnokov, V.I. Chepigin, V.A. Gorshkov, S. Hofmann, A.P. Kabachenko, M. Keters, A.Yu. Lavrentev, A.G. Popeko, J. Roháč, R.N. Sagaidak, Š. Šáro, A.V. Yeremin, Nucl. Instrum. Methods A **440**, 86 (2000).
35. K.-H. Schmidt, Z. Phys. A **316**, 19 (1984).
36. G.M. Ter-Akopyan, A.S. Iljinov, Yu.Ts. Oganessian, O.A. Orlova, G.S. Popeko, S.P. Tretyakova, V.I. Chepigin, B.V. Shilov, G.N. Flerov, Nucl. Phys. A **255**, 509 (1975).
37. A. Sobiczewski, private communication (2002).
38. M. Dahlinger, W. Bonin, E. Kankeleit, H. Backe, Nucl. Instrum. Methods Phys. Res. A **219**, 513 (1984).
39. R.N. Sagaidak, A.V. Yeremin, Nucl. Instrum. Methods Phys. Res. B **93**, 103 (1994).
40. A.G. Popeko, O.N. Malyshev, R.N. Sagaidak, A.V. Yeremin, Nucl. Instrum. Methods B **126**, 294 (1997).
41. R.N. Sagaidak, V.I. Chepigin, M.G. Itkis, A.P. Kabachenko, A.Yu. Lavarentev, O.N. Malyshev, Yu.Ts. Oganessian, A.G. Popeko, J. Rogac, A.V. Yeremin, G. Giardina, in *Proceedings of the International Conference on Nuclear Physics Nuclear Shells - 50 Years, Dubna, April 21-24, 1999*, edited by Yu.Ts. Oganessian, R. Kalpakchieva (World Scientific, Singapore, 2000), pp. 199–210.
42. A.V. Ignatyuk, G.N. Smirenkin, A.S. Tishin, Yad. Fiz., **21**, 485 (1975) (Sov. J. Nucl. Phys. **21**, 255 (1975)).
43. G. Audi, A.H. Wapstra, Nucl. Phys. A **595**, 509 (1995).
44. S. Cohen, F. Plasil, W.J. Swiatecki, Ann. Phys. (N.Y.) **82**, 557 (1974).
45. A.J. Sierk, Phys. Rev. C **33**, 2039 (1986).
46. W.D. Myers, W.J. Swiatecki, Nucl. Phys. A **601**, 141 (1996); LBL Preprint LBL-36803 (1994).
47. R.J. Charity, Phys. Rev. C **53**, 512 (1996).